*Post-print manuscript

https://doi.org/10.1080/14786419.2018.1499639

Graphical abstract

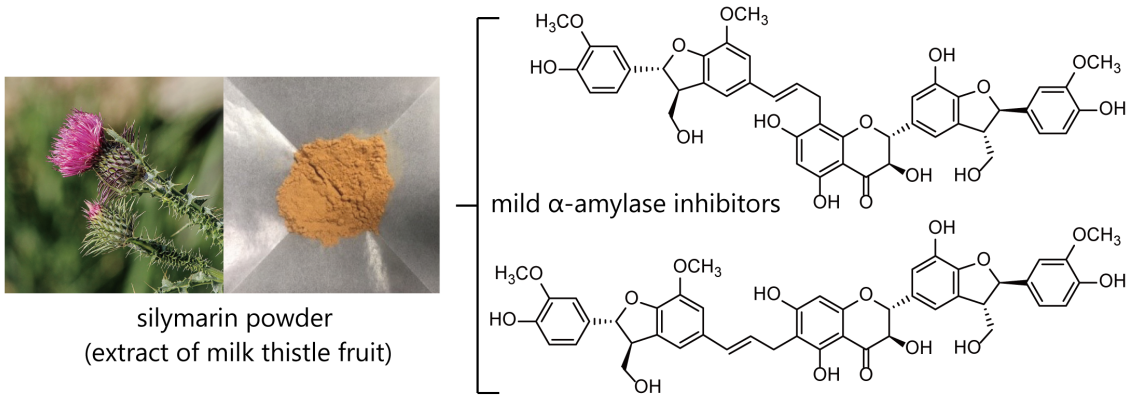

RESEARCH ARTICLE

Silychristin derivatives conjugated with coniferylalcohols from silymarin and their pancreatic α-amylase inhibitory activity

Eisuke Kato[a*], Natsuka Kushibiki[b], Hiroshi Satoh[c] and Jun Kawabata[a]

[a]*Division of Fundamental AgriScience and Research, Research Faculty of Agriculture, Hokkaido University, Kita-ku, Sapporo, Hokkaido 060-8589, Japan*

[b]*Division of Applied Bioscience, Graduate School of Agriculture, Hokkaido University, Kita-ku, Sapporo, Hokkaido 060-8589, Japan*

[c]*Nissei Bio Co. Ltd., Eniwa, Hokkaido, 061-1374, Japan*

***Corresponding author.** Eisuke Kato, [1]Division of Fundamental AgriScience and Research, Research Faculty of Agriculture, Hokkaido University, Kita-ku, Sapporo, Hokkaido 060-8589, Japan; Tel/Fax: +81 11 706 2496; e-mail: eikato@chem.agr.hokudai.ac.jp

Abstract

Silymarin is a mixture of flavonolignans extracted from the fruit of *Silybum marianum* (milk thistle). The latter is used as a medicinal plant to treat liver and gallbladder disorders. Recently, silymarin has been investigated for its effects against diabetes mellitus, and shown to reduce serum levels of glucose in model animals and in clinical trials. This effect can be explained mainly by the protective effect of silymarin against pancreatic beta-cells, but the involvement of other mechanisms is possible. We demonstrated the α-amylase inhibitory activity of silymarin and investigated the components responsible for this effect. Two major flavonolignans, silibinin and silychristin, did not show inhibition against α-amylase, but two novel silychristin derivatives conjugated with dehydrodiconiferyl alcohol were isolated as the mildly inhibiting components of silymarin. Further analyses indicated the presence of various silychristin derivatives in silymarin that may act synergistically to show α-amylase inhibitory activity.

Keywords: silymarin; milk thistle; α-amylase; diabetes mellitus

1. **Introduction**

Silymarin is a mixture of flavonoids extracted from the fruits of *Silybum marianum* (milk thistle). The latter was used by physicians in ancient Greece as a medicinal plant to treat disorders of the liver and gallbladder, as well as to protect liver against chemical and environmental toxins (Kren & Walterova 2005; Rainone 2005). Silymarin is the active component of milk thistle, and its effects against hepatic diseases and non-alcoholic fatty liver disease have been shown in several studies (Federico et al. 2017). Recent studies of silymarin have also reported its neuroprotective (Borah et al. 2013), renoprotective (Shahbazi et al. 2012), immunomodulative (Esmaeil et al. 2017), and cardioprotective effects (Razavi & Karimi 2016), thereby making it an interesting material for research.

Recently, silymarin has garnered attention for use against diabetes mellitus (DM) (Kazazis et al. 2014; Voroneanu et al. 2016; Stolf et al. 2017). DM is a metabolic disorder that causes an increase in the glucose level in blood. DM incidence has been increasing rapidly worldwide in recent years. A high amount of glucose in blood vessels leads to an increased risk of various complications. Therefore, the prevention and treatment of DM has been studied widely.

The effect of silymarin has been shown in several *in vivo* experiments against model animals and in clinical trials. Silymarin treatment to streptozotocin- or alloxan-induced DM in rats reduces serum levels of glucose and protects the pancreas (Soto et al. 2010; Amniattalab et al. 2016). Similar treatment with silymarin to partially

pancreatectomized rats also reduces serum levels of glucose compared with control, increases the insulin level, and induces the neogenesis of pancreatic beta-cells (C. Soto et al. 2014; Claudia Soto et al. 2014). Moreover, a trial of silymarin in DM patients reduced the levels of fasting blood glucose and glycated hemoglobin (Huseini et al. 2006). These positive effects of silymarin against DM could be attributed to its antioxidant and protective effects on pancreatic beta-cells. However, other effects may also contribute to the anti-DM property of silymarin, and the mechanism of action of silymarin is not completely explored.

Digestion of carbohydrates by glycosidases in the gastrointestinal tract is a target of anti-DM medications. Inhibition of α-amylase and α-glucosidase delays the digestion and absorption of carbohydrates, which reduces the rapid increase in the glucose level in blood after food consumption. These digestive enzymes are also studied as common targets of medicinal plants with anti-DM properties (Governa et al. 2018).

Here, we investigated if silymarin can modulate α-amylase activity and explored its active constituents. Silymarin showed inhibitory activity against α-amylase. However, silibinin (**1**) and silychristin (**2**), the major flavonolignans in silymarin (Csupor et al. 2016), were not shown to be α-amylase inhibitors. Investigation of the active components in silymarin led to the isolation of three novel silychristin derivatives (**4**–**6**) and mariamide B (**3**).

2. Results and Discussion

Silymarin showed inhibitory activity against pancreatic α-amylase in a

dose-dependent manner at 0.1–5 mg/mL (Figure S1).

To ascertain if the major flavonolignans contained in silymarin contribute to α-amylase inhibitory activity, silibinin (**1**, commercial, Sigma-Aldrich Co.) and silychristin (**2**, isolated, Cheng et al. 2013) were tested for their activity. However, silibinin (**1**) showed no inhibitory activity at <1.0 mg/mL, and nor did silychristin (**2**). Thus, activity-guided separation was undertaken to elucidate the component in silymarin with α-amylase inhibitory activity.

Silymarin was partitioned between solvents (water, 1-butanol, ethyl acetate). The ethyl-acetate layer was separated twice by silica-gel column chromatography to obtain the active fraction (AF). However, further separation of the AF by the reverse-phase column resulted in dispersed activity within broad range of fractions. This finding suggested that several compounds contribute to the α-amylase inhibitory activity of silymarin.

Next, we focused on analyzing the AF to explore the type of compound that contributes to α-amylase inhibition. The fractions obtained after reverse-phase column chromatography were analyzed by high-performance liquid chromatography (HPLC) and the major peaks were collected. The peaks were analyzed by nuclear magnetic resonance (NMR) and mass spectroscopy (MS) to elucidate their structures and these compounds were numbered **3**–**6** (Figure 1).

Compound **3** was obtained as a mixture which appeared as two peaks upon HPLC. These two peaks converted readily to each other and a single peak could not be

obtained, so they were analyzed as a mixture to elucidate their structures. Proton (^{1}H)-NMR suggested that the mixtures were *cis*/*trans* stereoisomers resulting from isomerization of an alkene moiety (*trans* isomer: 7.45/6.44 ppm, J = 15.5 Hz; *cis* isomer: 6.64/5.85 ppm, J = 12.7 Hz). Additional NMR procedures (^{13}C, correlated spectroscopy (COSY), heteronuclear multiple quantum coherence (HSQC) and heteronuclear multiple bond correlation (HMBC), Figure S4-S6) and comparison with the reported value (Choudhary et al. 2008; Qin et al. 2017) of predicted structures revealed compound **3** to be the mixture of mariamide B and its *trans*-isomer.

Compound **4** was analyzed by high resolution (HR)-electrospray ionization (ESI)-MS to reveal the molecular formula $C_{35}H_{32}O_{13}$ (found m/z 683.17583 $[M+Na]^+$, $C_{35}H_{32}O_{13}Na^+$ requires 683.17351). ^{1}H-NMR showed a similar spectrum to that of silychristin (**2**) but with additional signals indicating condensation of coniferyl alcohol. The predicted structure with the determined molecular formula did not correspond to any of the structures reported previously, thereby suggesting a novel compound. Careful analyses of compound **4** with ^{13}C-NMR, COSY, HSQC, and HMBC showed its structure (Table S1, Figure S7-S10)., which was named coniferylsilychristin (**4**)

Compounds **5** and **6** were analyzed by HR-ESI-MS to reveal the molecular formula $C_{45}H_{42}O_{15}$ (compound **5**: found m/z 845.24252 $[M+Na]^+$; compound **6**: found m/z 845.24139 $[M+Na]^+$; $C_{45}H_{42}O_{15}Na^+$ requires 845.24159). ^{1}H-NMR of compounds **5** and **6** showed a similar spectrum to that of silychristin (**2**) but with additional signals suggesting the conjugation of dehydrodiconiferyl alcohol, and compounds **5** and **6** were presumed to be novel compounds. Analyses of compounds **5** and **6** by ^{13}C-NMR, COSY, HSQC, and HMBC revealed their structures (Table S2,S3, Figure S11-S18), which were

named 8-dehydrodiconiferylsilychristin (**5**) and 6-dehydrodiconiferylsilychristin (**6**).

The isolated compounds were tested for their α-amylase inhibitory activity at 150–600 μM (Figure S2). Compounds **3** and **4** did not show concentration-dependent inhibition, thereby suggesting low contribution to the α-amylase inhibitory activity of silymarin. Compound **5** showed a mild but concentration-dependent with 50% inhibition at 600 μM, and compound **6** showed similar tendency but with slightly weaker activity with 38% inhibition at 600 μM.

Numbers of polyphenols including flavones, flavonols, and flavan-3-ols are reported for α-amylase inhibitory activity (Hara & Honda 1990; Piparo & Nestlé 2008; Sales et al. 2012). Their activity varies, which several compounds show potent activity (e.g. quercetin IC_{50}=21.4 μM, luteolin IC_{50}=18.4 μM) but other compounds show weak activity (e.g. epicatechin IC_{50}>1000 μM) which in some cases the maximum inhibition is limited. Compared to those compounds, compound **5** and **6** seems to be classified in the relatively weak group.

The results stated above showed that the isolated compounds (**3**–**6**) were not the principal components in silymarin, which is an α-amylase inhibitor. However, the isolation of novel silychristin derivatives (compounds **4**–**6**) suggested the presence of various silychristin derivatives in silymarin. In accordance with this hypothesis, we also identified several minor peaks of the AF with *m*/*z* 667 [taxifolin + dehydrodiconifenyl alcohol – H_2O + Na], 845 [silychristin + dehydrodiconifenyl alcohol – H_2O + Na], 985 [silychristin + silychristin – 2H + Na], 987 [silychristin + silychristin + Na] and 1165 [silychristin + silychristin + conifenyl alcohol – H_2O + Na]. These structures were not

determined due to low purities and low yields.

The interaction of a polyphenol and a protein correlates with the molecular size (Ozdal et al. 2013). Our previous study suggested that increased hydrophobic interactions have a positive correlation with α-amylase inhibition (Kato et al. 2011). Thus, dimerization of silychristin and condensation of coniferyl alcohol, which result in a larger molecular size and a larger area for hydrophobic interactions, are expected to confer higher α-amylase inhibitory activity to a compound. This hypothesis was also speculated from the present study because compounds **5** and **6**, with their larger molecular size, showed inhibitory activity but the smaller sized compounds **1**, **2** or **4** did not. Therefore, silychristin dimers and perhaps larger oligomers, with or without condensation of coniferyl alcohol, might be the active components that work synergistically to show α-amylase inhibitory activity in silymarin.

3. Experimental

See supplementary material for the experimental methods and spectral data of the isolated compounds.

4. Conclusions

We showed the α-amylase inhibitory activity of silymarin that may partake in the anti-DM effect of this well-known medicinal-plant extract. Silibinin (**1**) and silychristin (**2**), the two major flavonolignans, were not the components that work as α-amylase inhibitors in silymarin. Fractionation of silibinin revealed several novel silychristin derivatives (compounds **4**–**6**) in this flavonolignan mixture, and the presence

of additional related compounds was indicated from MS. Although each of the compounds showed low or mild α-amylase inhibitory activity, these silychristin derivatives may potentially work synergistically to reveal the α-amylase inhibitory activity of silymarin.

Acknowledgements

We thank Global Facility Center, Hokkaido University for measurement of HR-ESI-MS and Dr. Eri Fukushi of the GC-MS and NMR Laboratory, Faculty of Agriculture, Hokkaido University, for the advice regarding NMR measurements. We thank Arshad Makhdum, PhD, from Edanz Group (www.edanzediting.com/ac) for editing a draft of this manuscript.

References

Amniattalab A, Malekinejad H, Rezabakhsh A, Rokhsartalab-Azar S, Alizade-Fanalou S. 2016. Silymarin: A Novel Natural Agent to Restore Defective Pancreatic β Cells in Streptozotocin (STZ)-induced Diabetic Rats. Iran J Pharm Res. 15:493–500.

Borah A, Paul R, Choudhury S, Choudhury A, Bhuyan B, Das Talukdar A, Dutta Choudhury M, Mohanakumar KP. 2013. Neuroprotective Potential of Silymarin against CNS Disorders: Insight into the Pathways and Molecular Mechanisms of Action. CNS Neurosci Ther. 19:847–853.

Cheng X-R, Jie R, Wang C-H, Guan B, Jin H-Z, Zhang W-D. 2013. Chemical Constituents from Inula wissmanniana. Chem Nat Compd. 49:815–818.

Choudhary MI, Begum A, Abbaskhan A, Musharraf SG, Ejaz A, Atta-ur-Rahman. 2008. Two New Antioxidant Phenylpropanoids from Lindelofia stylosa. Chem Biodivers. 5:2676–2683.

Csupor D, Csorba A, Hohmann J. 2016. Recent advances in the analysis of flavonolignans of Silybum marianum. J Pharm Biomed Anal. 130:301–317.

Esmaeil N, Anaraki SB, Gharagozloo M, Moayedi B. 2017. Silymarin impacts on immune system as an immunomodulator: One key for many locks. Int Immunopharmacol. 50:194–201.

Federico A, Dallio M, Loguercio C. 2017. Silymarin/Silybin and Chronic Liver Disease: A Marriage of Many Years. Molecules. 22:191.

Governa P, Baini G, Borgonetti V, Cettolin G, Giachetti D, Magnano A, Miraldi E, Biagi M. 2018. Phytotherapy in the Management of Diabetes: A Review. Molecules. 23:105.

Hara Y, Honda M. 1990. The Inhibition of α-Amylase by Tea Polyphenols. Agric Biol Chem. 54:1939–1945.

Huseini HF, Larijani B, Heshmat R, Fakhrzadeh H, Radjabipour B, Toliat T, Raza M. 2006. The efficacy of Silybum marianum (L.) Gaertn. (silymarin) in the treatment of type II diabetes: a randomized, double-blind, placebo-controlled, clinical trial. Phyther Res. 20:1036–1039.

Kato E, Iwano N, Yamada A, Kawabata J. 2011. Synthesis and α-amylase inhibitory activity of glucose-deoxynojirimycin conjugates. Tetrahedron. 67:7692–7702.

Kazazis CE, Evangelopoulos AA, Kollas A, Vallianou NG. 2014. The Therapeutic Potential of Milk Thistle in Diabetes. Rev Diabet Stud. 11:167–174.

Kren V, Walterova D. 2005. Silybin and silymarin - new effects and applications. Biomed Pap. 149:29–41.

Ozdal T, Capanoglu E, Altay F. 2013. A review on protein–phenolic interactions and associated changes. Food Res Int. 51:954–970.

Piparo E Lo, Nestlé SA. 2008. Flavonoids for controlling starch digestion : Structural requirements for inhibiting human Flavonoids for Controlling Starch Digestion : Structural Requirements for Inhibiting Human α-Amylase. J Med Chem. 51:3555–3561.

Qin N bo, Jia C cui, Xu J, Li D hong, Xu F xing, Bai J, Li Z lin, Hua H ming. 2017. New amides from seeds of Silybum marianum with potential antioxidant and antidiabetic activities. Fitoterapia. 119:83–89.

Rainone F. 2005. Milk thistle. Am Fam Physician. 72:1285–8.

Razavi BM, Karimi G. 2016. Protective effect of silymarin against chemical-induced cardiotoxicity. Iran J Basic Med Sci. 19:916–923.

Sales PM, Souza PM, Simeoni LA, Silveira D. 2012. α-Amylase inhibitors: a review of raw material and isolated compounds from plant source. J Pharm Pharm Sci. 15:141–83.

Shahbazi F, Dashti-Khavidaki S, Khalili H, Lessan-Pezeshki M. 2012. Potential Renoprotective Effects of Silymarin Against Nephrotoxic Drugs: A Review of Literature. J Pharm Pharm Sci. 15:112–123.

Soto C, Pérez J, García V, Uría E, Vadillo M, Raya L. 2010. Effect of silymarin on kidneys of rats suffering from alloxan-induced diabetes mellitus. Phytomedicine. 17:1090–1094.

Soto C, Raya L, Juárez J, Pérez J, González I. 2014. Effect of Silymarin in Pdx-1 expression and the proliferation of pancreatic β-cells in a pancreatectomy model. Phytomedicine. 21:233–239.

Soto C, Raya L, Pérez J, González I, Pérez S. 2014. Silymarin Induces Expression of Pancreatic Nkx6.1 Transcription Factor and β-Cells Neogenesis in a Pancreatectomy Model. Molecules. 19:4654–4668.

Stolf AM, Cardoso CC, Acco A. 2017. Effects of Silymarin on Diabetes Mellitus Complications: A Review. Phyther Res. 31:366–374.

Voroneanu L, Nistor I, Dumea R, Apetrii M, Covic A. 2016. Silymarin in Type 2 Diabetes Mellitus: A Systematic Review and Meta-Analysis of Randomized Controlled Trials. J Diabetes Res. 2016:1–10.

Figure

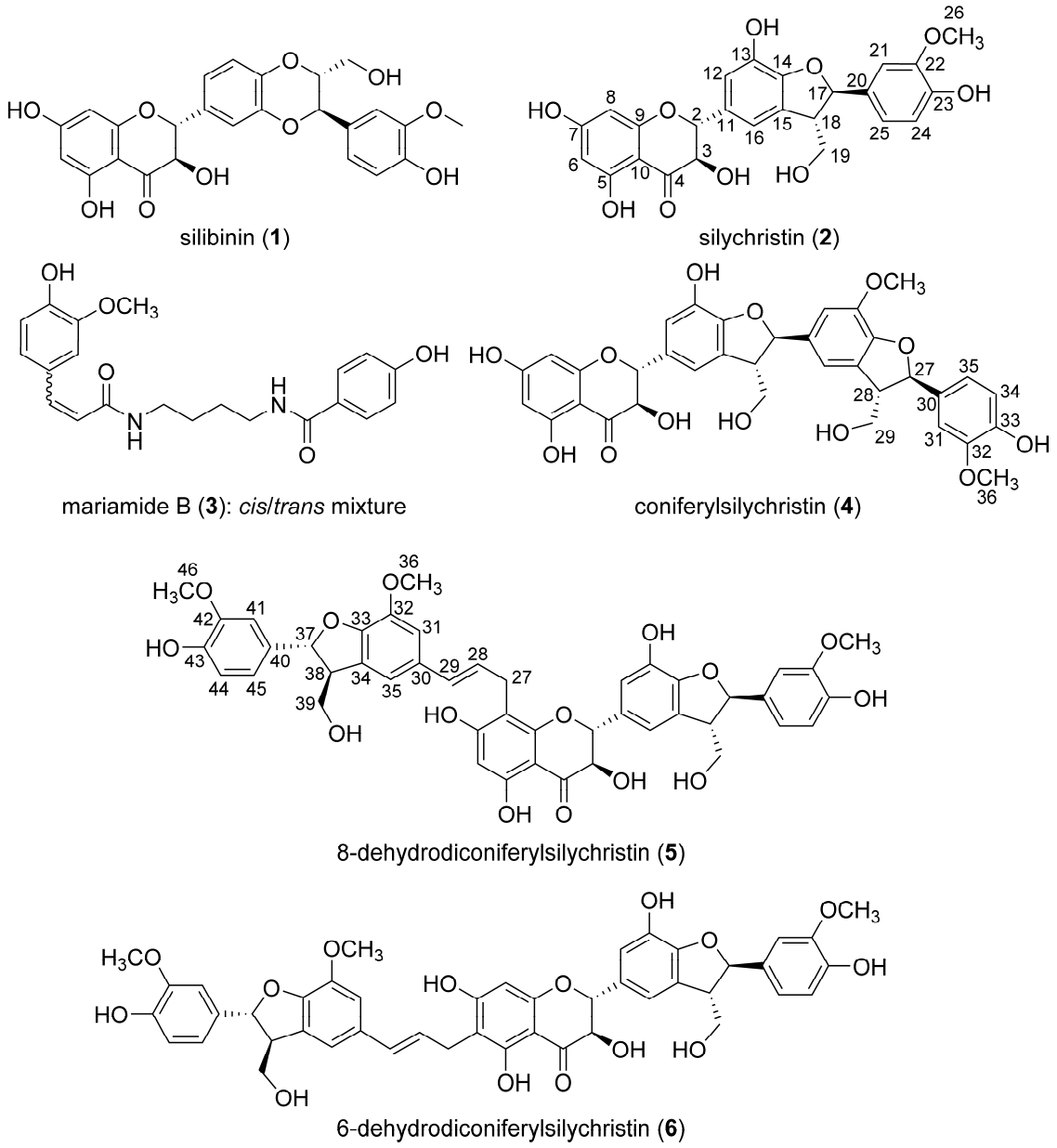

Figure 1. Structure of compounds. Stereochemical relationship between central silychristin core and additional *trans*-dihydrofuran moieties are not determined in compounds **4**–**6**.

SUPPLEMENTARY MATERIAL

Silychristin derivatives conjugated with coniferylalcohols from silymarin and their pancreatic α-amylase inhibitory activity

Eisuke Kato[a*], Natsuka Kushibiki[b], Hiroshi Satoh[c] and Jun Kawabata[a]

[a]*Division of Fundamental AgriScience and Research, Research Faculty of Agriculture, Hokkaido University, Kita-ku, Sapporo, Hokkaido 060-8589, Japan*

[b]*Division of Applied Bioscience, Graduate School of Agriculture, Hokkaido University, Kita-ku, Sapporo, Hokkaido 060-8589, Japan*

[c]*Nissei Bio Co. Ltd., Eniwa, Hokkaido, 061-1374, Japan*

***Corresponding author.** Eisuke Kato, [1]Division of Fundamental AgriScience and Research, Research Faculty of Agriculture, Hokkaido University, Kita-ku, Sapporo, Hokkaido 060-8589, Japan; Tel/Fax: +81 11 706 2496; e-mail: eikato@chem.agr.hokudai.ac.jp

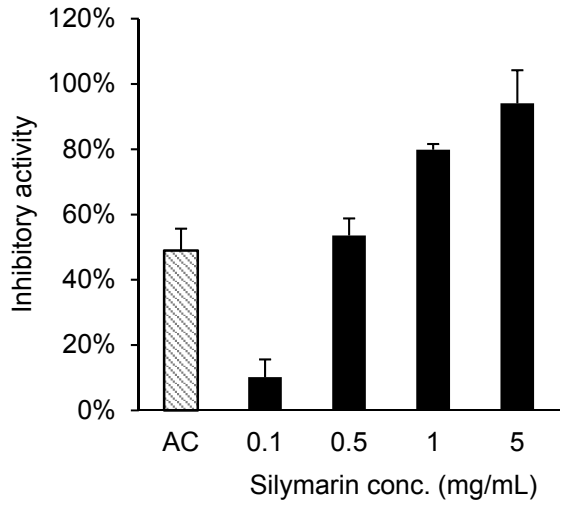

Figure S1. α-amylase inhibitory activity of silymarin. AC: acarbose (10 μM)

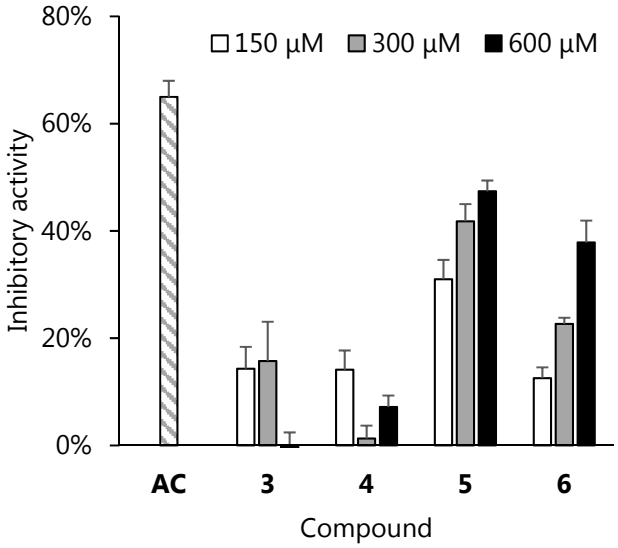

Figure S2. α-amylase inhibitory activity of isolated compounds. AC: acarbose (10 μM)

Experimental

General

Silymarin (a mixture of flavonolignans extracted from the fruits of milk thistle) was obtained from Omnica Co., Ltd. (Tokyo, Japan). Silibinin was purchased from Sigma–Aldrich Japan K. K. (Tokyo, Japan). All other chemicals were from Wako Pure Chemical Industries, Ltd. (Osaka, Japan) unless stated otherwise. Absorbance was measured using a Synergy™ MX microplate reader (BioTek Instruments, Inc., Winooski, VT, USA). An AMX 500 system (Bruker Japan K.K., Yokohama, Japan) was used to obtain NMR spectra, and residual solvents were used as an internal standard (acetone-d_6: ^{1}H 2.04 ppm, ^{13}C 29.92 ppm; methanol-d_4: ^{1}H 3.30 ppm, ^{13}C 49.00 ppm). A LCT Premier Spectrometer (Nihon Waters K.K., Tokyo, Japan) was employed to obtain low-resolution mass spectra and an Exactive system (Thermo Fisher Scientific K.K., Tokyo, Japan) was used for HR-ESI-MS.

Measurement of α-amylase inhibitory activity

The α-amylase inhibitory activity was determined using starch azure (Sigma–Aldrich; S7629) as the substrate and porcine pancreatic α-amylase (Sigma–Aldrich; A3176) as the enzyme. Briefly, 350 μL of starch azure (4 mg/mL) suspended in Tris-HCl buffer (0.1 M, pH 6.9, 0.01 M $CaCl_2$), 100 μL of sample dissolved in water, and 50 μL of porcine pancreatic α-amylase dissolved in Tris-HCl buffer were incubated with frequent mixing for 10 min at 37°C. The reaction was stopped by addition of 50% acetic acid (50 μL) and centrifugation (1,500 × *g*, 5 min). The absorbance at 595 nm of the supernatant was measured. Absorbance of the blank (without enzyme) was subtracted and inhibitory activity was calculated compared with that of the control value. Each experiment was carried out in duplicate and repeated at least twice. Mean values are shown in the figures.

Isolation procedure

Silymarin powder (30 g) was suspended in water and extracted by ethyl acetate and then 1-butanol to obtain a layer of water (1.0 g), 1-butanol (3.73 g), and ethyl acetate (20.1 g). The ethyl-acetate layer (10.86 g) was loaded on a silica-gel column (5.0 × 25.0 cm) and eluted stepwise by

chloroform/methanol = 20/1, 10/1, 5/1, 0/1 (1.5-L each). The fractions eluted by chloroform/methanol = 5/1, 0/1 (5.84 g) were combined and purified again by silica-gel column chromatography (5.0 × 22.0 cm), and eluted stepwise by hexane/ethyl acetate = 1/2, 1/3, 1/6 and then by acetone (1.2-L each). Silychristin (**2**) was isolated from the fraction eluted by hexane/ethyl acetate = 1/2 and 1/3 using preparative thin-layer chromatography (hexane/ethyl acetate = 1/6 with 5% acetic acid) (Figure S3). The fraction eluted by acetone (AF, 1.53 g out of 1.86 g) was purified by reverse-phase column chromatography using a Cosmosil 75C_{18}-OPN column (3.0 × 22.0 cm; Nakalai Tesque, Inc., Kyoto, Japan) and eluted stepwise by methanol/water = 3/7, 5/5, 6/4, 7/3, 8/2 with 0.1% trifluoroacetic acid (TFA) (500-mL each, fraction named AF-1 to AF-5).

Fractions AF-1 and 2 were combined (410 mg) and loaded onto a Sephadex LH-20 column (1.5 × 27.0 cm; GE Healthcare Japan Co., Tokyo, Japan) for column chromatography and eluted by methanol, and divided into six fractions (100-mL each, AF-1/2-1 to AF-1/2-6). AF-1/2-3 (83 mg) was purified by HPLC [column: Cosmosil πNAP (10 × 250 mm); mobile phase: gradient elution from 40% aq. methanol with 0.1% TFA to 95% aq. methanol with 0.1% TFA (0–60 min)] to obtain compound **3** (2.2 mg). AF-1/2-5 (97.1 mg) was purified by HPLC [column: Cosmosil πNAP (10 × 250 mm); mobile phase: gradient elution from 40% aq. methanol with 0.1% TFA to 95% aq. methanol with 0.1% TFA (0–60 min)] to obtain a peak. The peak was purified by HPLC [column: Cosmosil PBr (10 × 250 mm, Nakalai Tesque, Inc.); mobile phase: 70 aq. methanol with 0.1% TFA] to obtain compound **4** (3.3 mg).

Fraction AF-3 (325.3 mg) was purified by HPLC [column: Cosmosil πNAP (10 × 250 mm, Nakalai Tesque, Inc.); mobile phase: 65% aq. methanol with 0.1% TFA] to obtain two major peaks. Each peak was purified by HPLC [column: Cosmosil πNAP (10 × 250 mm); mobile phase: 40% aq. acetonitrile with 0.1% TFA] to obtain compounds **5** (3.0 mg) and **6** (4.8 mg).

Data of the isolated compounds

Silychristin A (**2**): ^{1}H-NMR (500 MHz, rt, methanol-d_4) 3.53 (1H, dt, *J*=6.2, 6.1 Hz), 3.83 (3H, s), 3.80-3.87 (2H, m),

4.54 (1H, d, *J*=11.5 Hz), 4.94 (1H, d, *J*=11.5 Hz), 5.56 (1H, d, *J*=6.2 Hz), 5.88 (1H, d, *J*=2.1 Hz), 5.92 (1H, d, *J*=2.1 Hz), 6.77 (1H, d, *J*=8.2 Hz), 6.86 (1H, dd, *J*=1.8, 8.2 Hz), 6.90 (1H, d, *J*=1.6 Hz), 6.95 (1H, br s), 6.99 (1H, d, *J*=1.8 Hz) ppm; ^{13}C-NMR (125 MHz, rt, methanol-d_4) 55.53, 56.41, 64.82, 73.76, 85.29, 89.11, 96.29, 97.35, 101.84, 110.60, 116.15, 116.63, 116.93, 119.76, 130.10, 131.59, 134.75, 142.17, 147.53, 149.12, 149.12, 164.49, 165.33, 168.74, 198.35 ppm; ESI-MS (positive) *m*/*z*=505 $[M+Na]^+$.

Data was compared with the reported values (Cheng et al. 2013).

Mariamide B (**3**): colorless solid, cis-isomer ^{1}H-NMR (500 MHz, rt, methanol-d_4) 1.55-1.60 (4H, m), 3.22-3.37 (4H, m), 3.81 (3H, s), 5.83 (1H, d, *J*=12.7 Hz), 6.61 (1H, d, *J*=12.7 Hz), 6.73 (1H, d, *J*=8.2 Hz), 6.82 (2H, d, *J*=8.4 Hz), 6.93 (1H, dd, *J*=1.3, 8.2 Hz), 7.35 (1H, d, *J*=1.3 Hz), 7.67-7.70 (2H, m) ppm; ^{13}C-NMR (125 MHz, rt, methanol-d_4) 27.70, 27.97, 40.10, 40.48, 56.39, 113.93, 115.82, 116.04, 116.04, 121.78, 124.78, 126.56, 128.61, 130.19, 130.19, 138.22, 148.51, 148.51, 161.95, 170.11, 170.46 ppm; trans-isomer ^{1}H-NMR (500 MHz, rt, methanol-d_4) 1.60-1.69 (4H, m), 3.30-3.42 (4H, m), 3.88 (3H, s), 6.42 (1H, d, *J*=15.8 Hz), 6.79 (1H, d, *J*=8.1 Hz), 6.80 (2H, d, *J*=8.4 Hz), 7.02 (1H, dd, *J*=1.0, 8.1 Hz), 7.11 (1H, d, *J*=1.0 Hz), 7.43 (1H, d, *J*=15.8 Hz), 7.67-7.70 (2H, m) ppm; ^{13}C-NMR (125 MHz, rt, methanol-d_4) 28.03, 28.05, 40.22, 40.50, 56.39, 111.55, 116.04, 116.04, 116.47, 118.77, 123.19, 126.56, 128.29, 130.19, 130.19, 142.00, 149.29, 149.82, 161.95, 169.23, 170.11 ppm; ESI-MS (positive) *m*/*z*=385 $[M+H]^+$.

Data was compared with the reported values (Choudhary et al. 2008; Qin et al. 2017).

Coniferylsilychristin (**4**): brown solid, see Table S1 for NMR data. HR-ESI-MS (positive): found *m*/*z* 683.17583 $[M+Na]^+$, $C_{35}H_{32}O_{13}Na^+$ requires 683.17351; IR (neat) ν = 726, 783, 849, 1030, 1089, 1145, 1206, 1278, 1343, 1465, 1498, 1516, 1635, 1677, 2285, 2349, 2925, 3376 cm^{-1}; $[\alpha]_D^{23}$ +52.7° (c = 0.073, methanol).

8-dehydrodiconyferylsilychristin (**5**): brown solid, see Table S2 for NMR data. HR-ESI-MS (positive): found *m*/*z* 845.24252 $[M+Na]^+$, $C_{45}H_{42}O_{15}Na^+$ requires 845.24159; IR (neat) ν = 1158, 1212, 1278, 1339, 1361, 1436, 1456, 1498, 1517, 1541, 1558, 1636, 1684, 1698, 2882, 2938, 3239, 3319, 3363, 3376, 3567, 3588, 3609, 3629 cm^{-1}; $[\alpha]_D^{27}$ +62.0° (c = 0.132, acetone).

6-dehydrodiconyferylsilychristin (**6**): brown solid, see Table S3 for NMR data. HR-ESI-MS (positive): found *m*/*z* 845.24139 $[M+Na]^+$; $C_{45}H_{42}O_{15}Na^+$ requires 845.24159; IR (neat) ν = 780, 816, 861, 967, 1033, 1090, 1121, 1145, 1208, 1274, 1341, 1453, 1497, 1518, 1636, 3381 cm^{-1}; $[\alpha]_D^{24}$ +71.0° (c = 0.400, acetone).

NMR data of compound 4-6

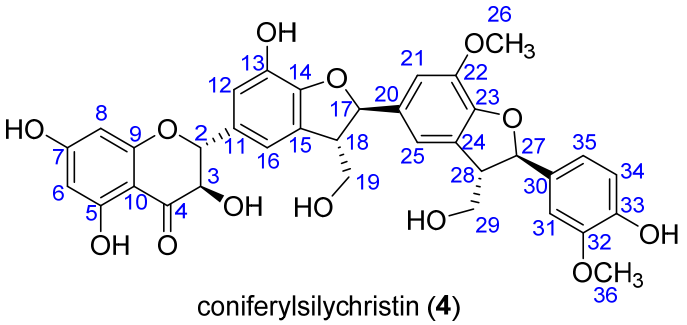

coniferylsilychristin (**4**)

Table S1. NMR data of compound **4** (500 MHz, rt, methanol-d_4)

No.	^{1}H	^{13}C	No.	^{1}H	^{13}C
2	4.94 (d, *J*=11.4)	85.27	20	-	136.84
3	4.54 (d, *J*=11.4)	73.78	21	6.97 (s)	112.04
4	-	198.31	22	-	145.50
5	-	165.33	23	-	149.35
6	5.92 (d, *J*=1.4)	97.39	24	-	130.41
7	-	168.75	25	6.97 (s)	115.82
8	5.88 (d, *J*=1.4)	96.32	26	3.85 (s)	56.91
9	-	164.50	27	5.53 (d, *J*=6.3)	89.29
10	-	101.86	28	3.49 (dt, *J*=6.3, 5.9)	55.30
11	-	131.64	29	3.74-3.83 (2H, m)	64.88
12	6.91 (br s)	117.00	30	-	134.62
13	-	142.19	31	6.94 (d, *J*=1.3)	110.71
14	-	149.11	32	-	149.14
15	-	130.10	33	-	147.63
16	6.95 (br s)	116.62	34	6.76 (d, *J*=8.2)	116.22
17	5.60 (d, *J*=6.3)	89.29	35	6.82 (dd, *J*=1.3, 8.2)	119.75
18	3.57 (dt, *J*=6.3, 5.8)	55.56	36	3.81 (s)	56.47

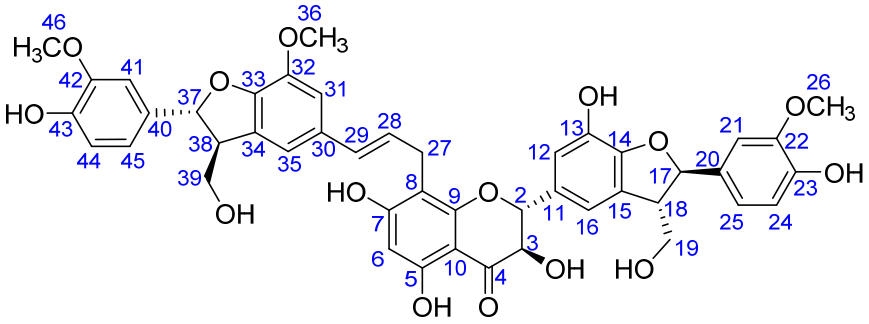

8-dehydrodiconiferylsilychristin (**5**)

Table S2. NMR data of compounds **5** (500 MHz, rt, acetone-d_6)

No.	^{1}H	^{13}C	No.	^{1}H	^{13}C
2	5.07 (d, *J*=11.4)	84.56	25	6.92 (dd, *J*=1.3, 8.2)	119.84
3	4.57 (d, *J*=11.4)	73.52	26	3.80 (s)[a]	56.33[b]
4	-	198.44	27	3.33 (dd, *J*=6.0, 14.3)	26.32
				3.39 (dd, *J*=6.0, 14.3)	
5	-	162.91	28	6.13 (td, *J*=6.0, 15.8)	126.16
6	6.12 (s)	96.77	29	6.30 (d, *J*=15.8)	131.10
7	-	165.64	30	-	132.55
8	-	107.31	31	6.84 (br s)	111.38
9	-	161.18	32	-	145.15
10	-	101.60	33	-	148.64
11	-	131.68	34	-	130.34
12	7.05 (br s)	116.77	35	6.90 (br s)	115.69
13	-	141.75	36	3.81 (s)	56.38
14	-	148.48	37	5.51 (d, *J*=6.3)	88.43
15	-	130.11	38	3.48 (dt, *J*=6.0, 6.0)	54.73
16	7.07 (br s)	116.22	39	3.78-3.90 (m)	64.51
17	5.57 (d, *J*=6.6)	88.73	40	-	134.41
18	3.59 (dt, *J*=6.0, 6.0)	55.08	41	7.00 (br s)	110.56
19	3.78-3.90 (m)	64.43	42	-	148.48
20	-	134.25	43	-	147.31
21	7.10 (br s)	110.66	44	6.79 (d, *J*=8.2)	115.75
22	-	148.45	45	6.85 (d, *J*=8.2)	119.65
23	-	147.33	46	3.82 (s)[a]	56.42[b]
24	6.82 (d, *J*=8.2)	115.75	5-OH	11.67 (s)	

Note: a–b: values with the same superscript may be interchanged.

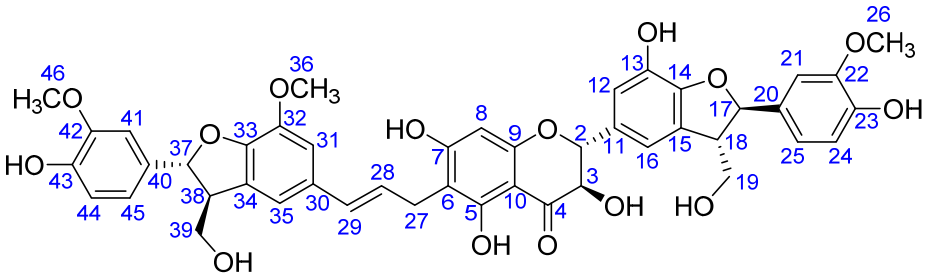

6-dehydrodiconiferylsilychristin (**6**)

Table S3. NMR data of compounds 6 **(500 MHz, rt, acetone-d_6)**

No.	^{1}H	^{13}C	No.	^{1}H	^{13}C
2	5.01 (d, *J*=11.7)	84.85	25	6.85 (dd, *J*=1.3, 8.2)	119.63
3	4.63 (d, *J*=11.7)	73.39	26	3.79 (s)	56.32
4	-	198.42	27	3.42 (2H, d, *J*=6.5)	25.91
5	-	162.11[c]	28	6.19 (dt, *J*=6.5, 15.7)	126.1
6	-	108.07	29	6.37 (d, *J*=15.7)	130.98
7	-	165.66	30	-	132.59
8	6.08 (s)	95.62	31	6.86 (br s)	111.35
9	-	162.15[c]	32	-	145.16
10	-	101.4	33	-	148.60[d]
11	-	131.35	34	-	130.13
12	6.98 (br s)	116.84	35	6.90 (br s)	115.67
13	-	141.8	36	3.82 (s)	56.38
14	-	148.62[d]	37	5.57 (d, *J*=6.4)	88.64
15	-	130.35	38	3.58 (dt, *J*=6.4, 6.2)	55.08
16	7.00 (br s)	116.58	39	3.78-3.91 (m)	64.5
17	5.52 (d, *J*=6.4)	88.47	40	-	134.31
18	3.50 (dt, *J*=6.4, 6.2)	54.82	41	7.07 (d, *J*=1.3)	110.68
19	3.78-3.91 (m)	64.57	42	-	148.43[e]
20	-	134.47	43	-	147.30[f]
21	7.00 (br s)	110.56	44	6.81 (d, *J*=7.8)	115.74
22	-	148.47[e]	45	6.91 (dd, *J*=1.3, 7.8)	119.78
23	-	147.35[f]	46	3.82 (s)	56.38
24	6.78 (d, *J*=8.2)	115.74	5-OH	12.03 (s)	

Note: c–f: values with the same superscript may be interchanged.

NMR spectrums
Silychristin (2)

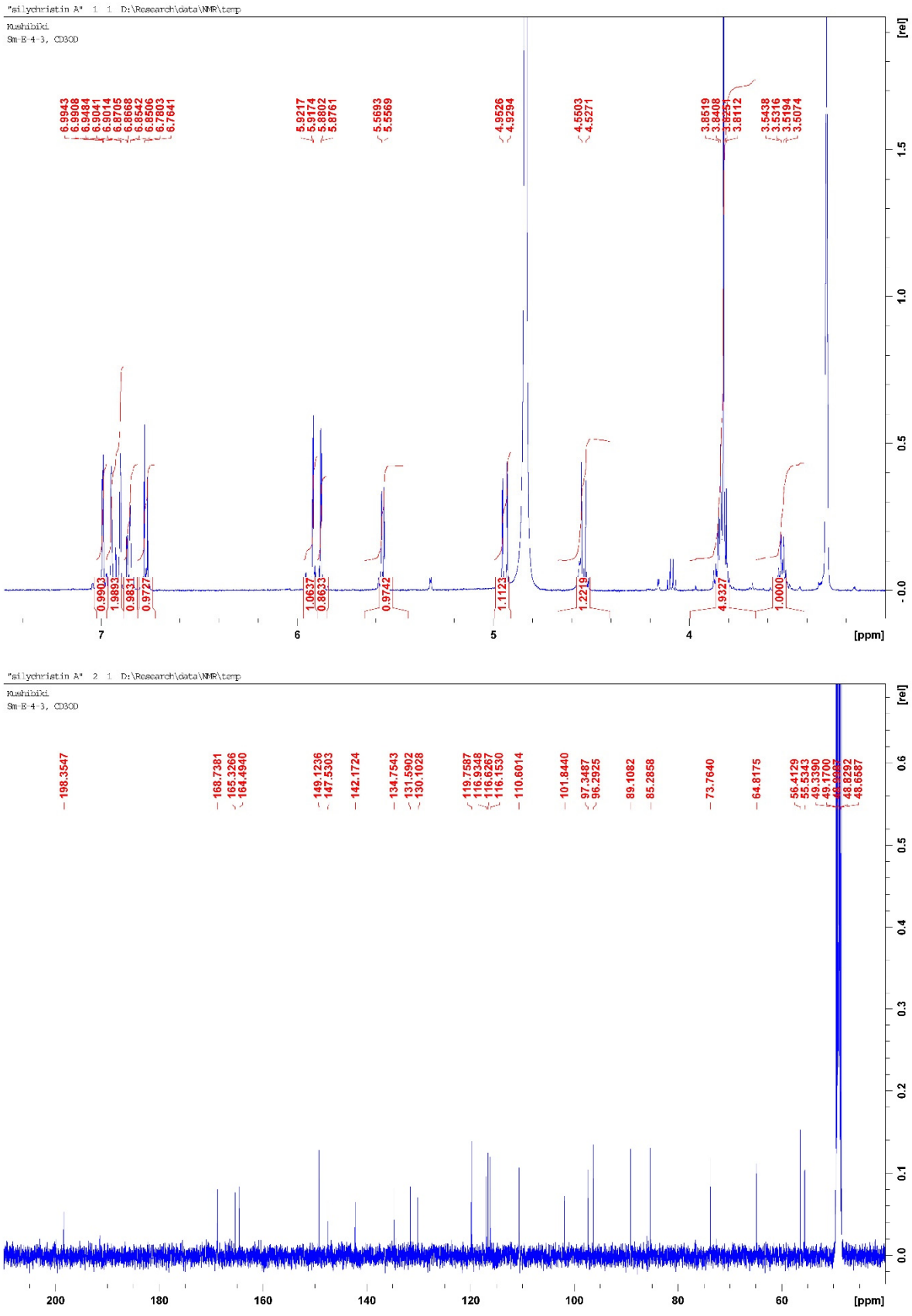

Figure S3. ^{1}H, ^{13}C-NMR spectrum of silychristin (**2**)

Mariamide B (3, cis/trans mixture)

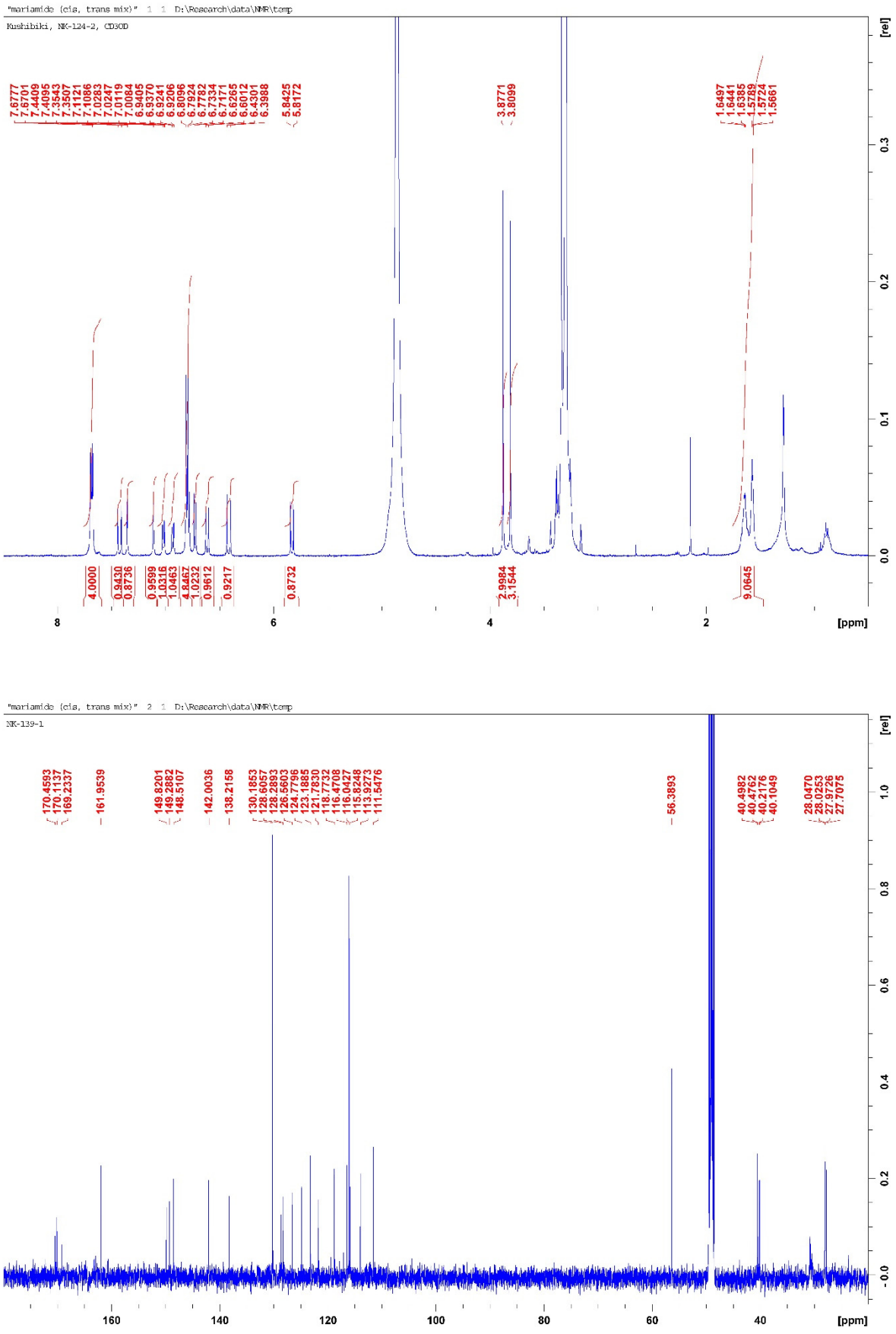

Figure S4. ^{1}H, ^{13}C-NMR spectrum of mariamide B (**3**, *cis*/*trans* mixture)

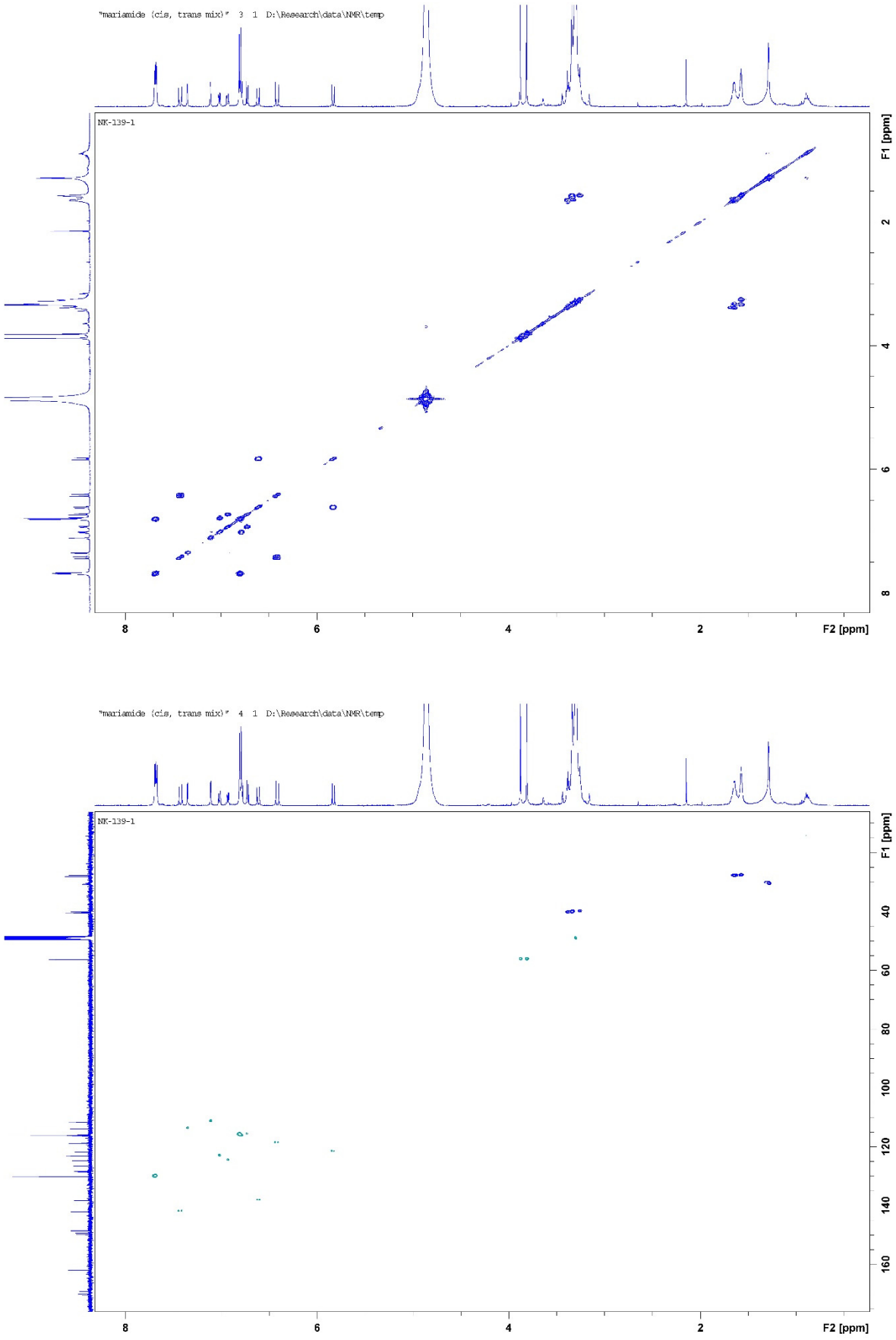

Figure S5. H-H COSY, HSQC spectrum of mariamide B (**3**, *cis*/*trans* mixture)

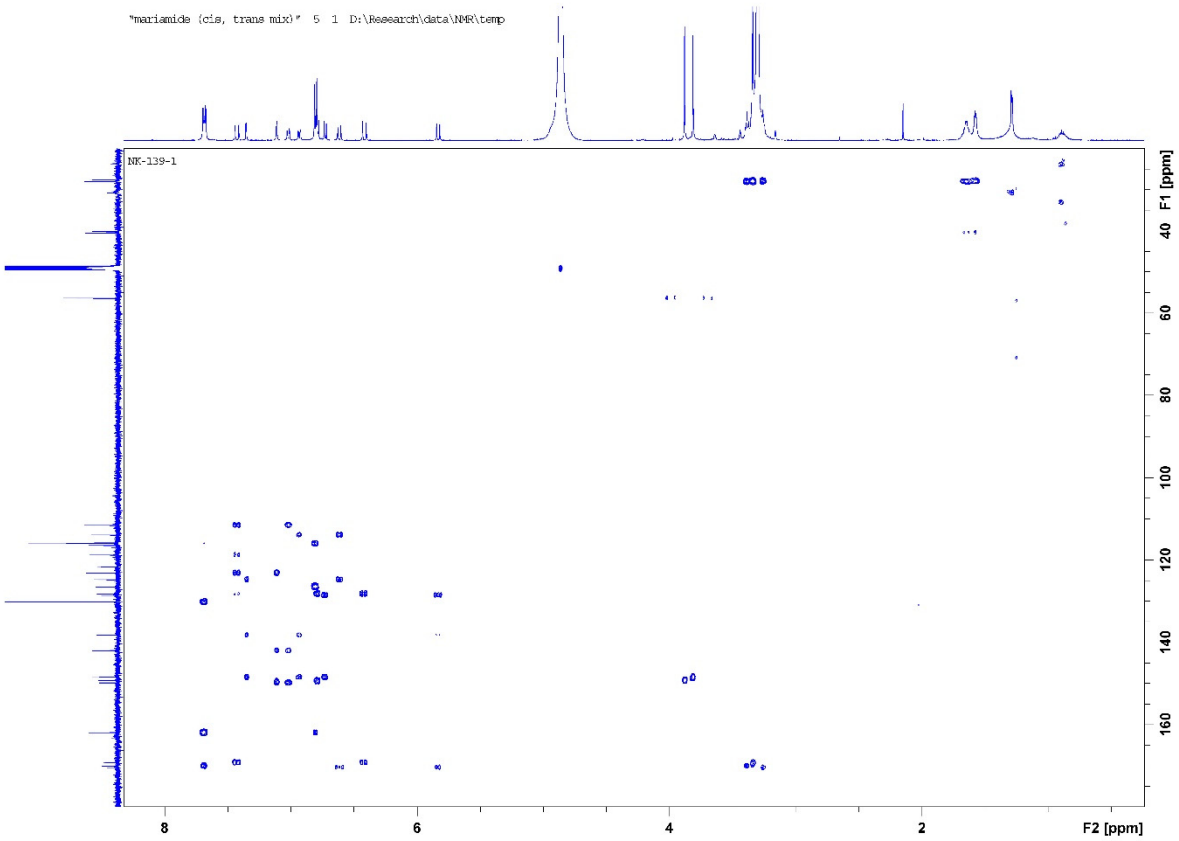

Figure S6. HMBC spectrum of mariamide B (**3**, *cis*/*trans* mixture)

Coniferylsilychristin (4)

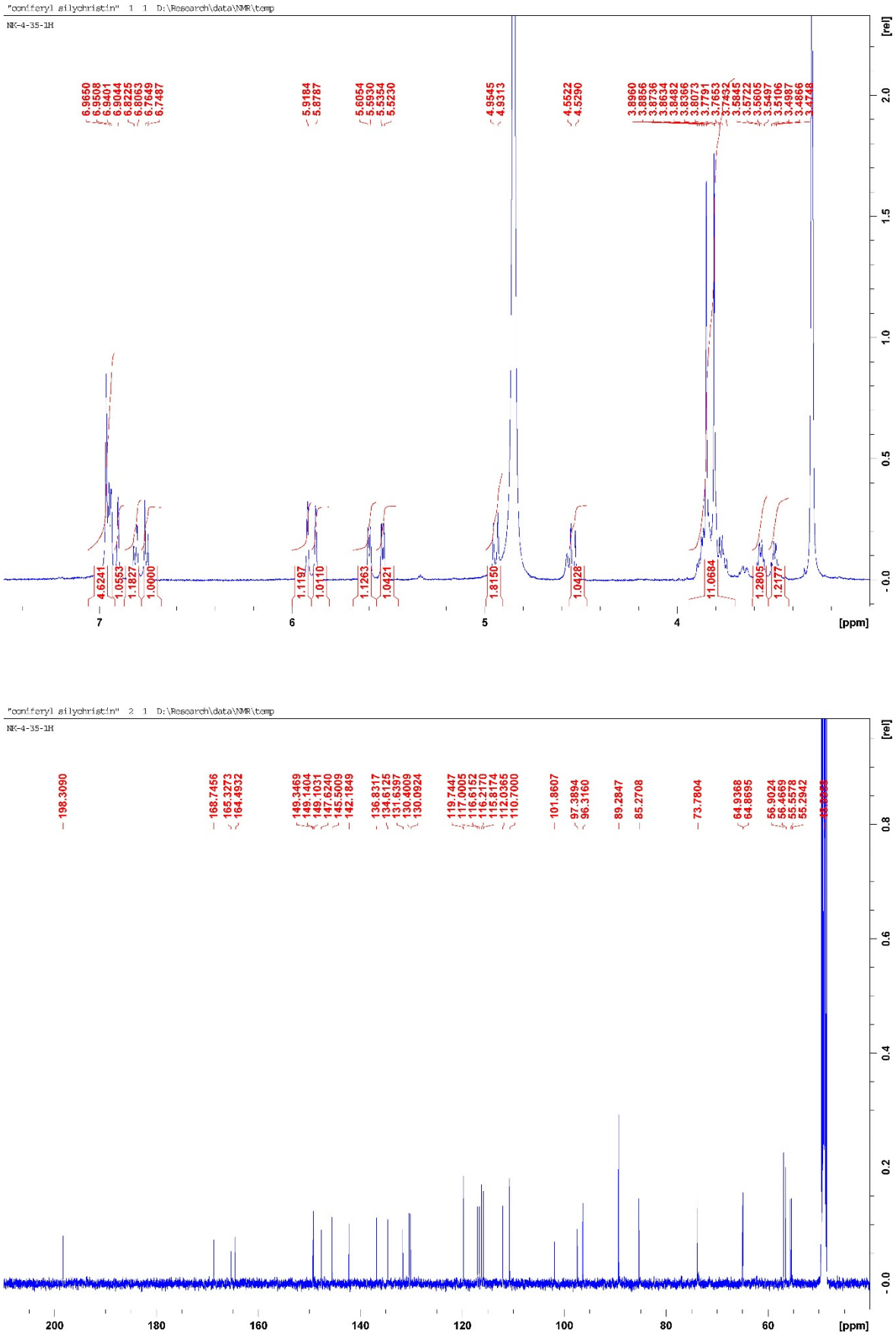

Figure S7. ^{1}H, ^{13}C-NMR spectrum of coniferylsilychristin (**4**)

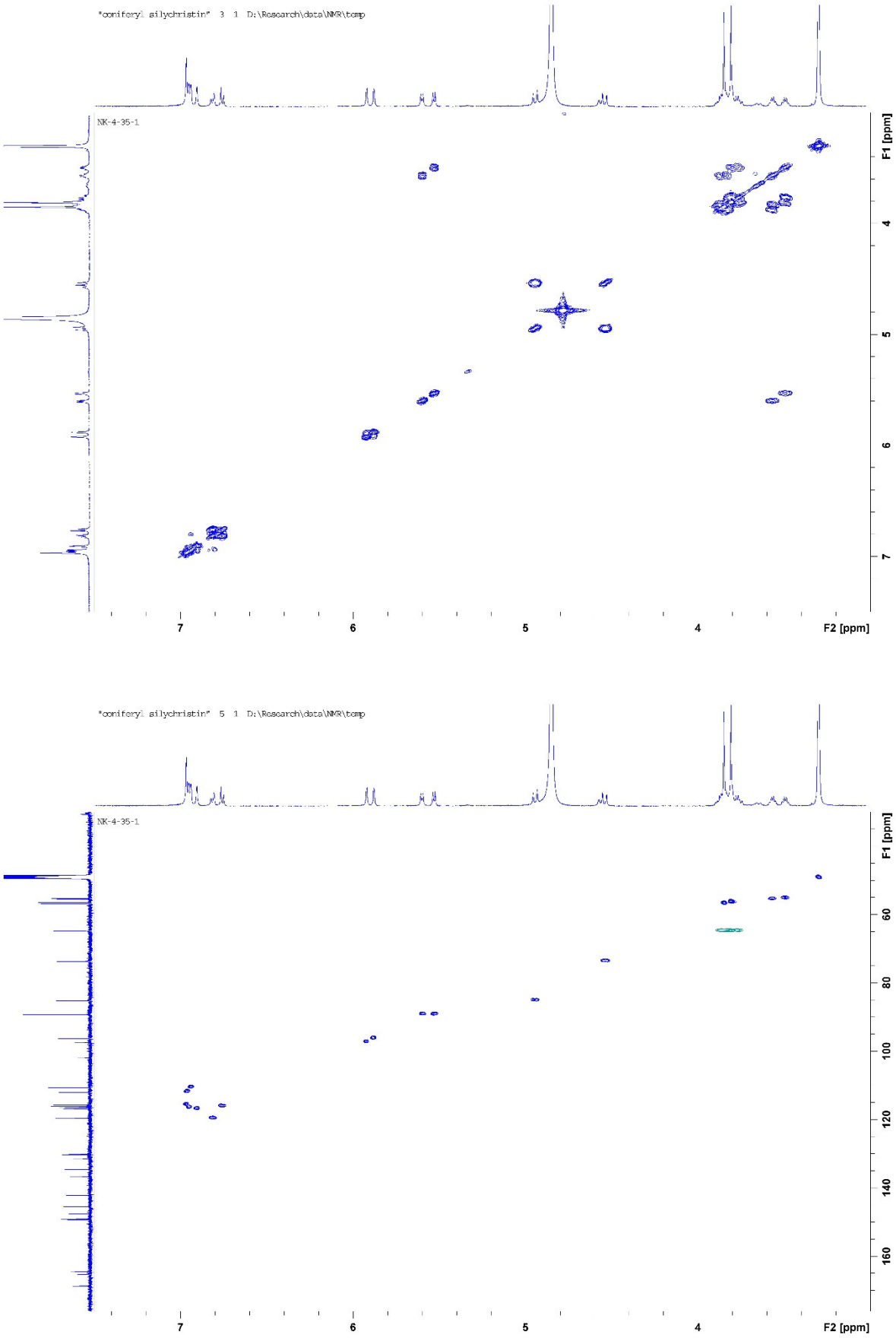

Figure S8. H-H COSY, HSQC spectrum of coniferylsilychristin (**4**)

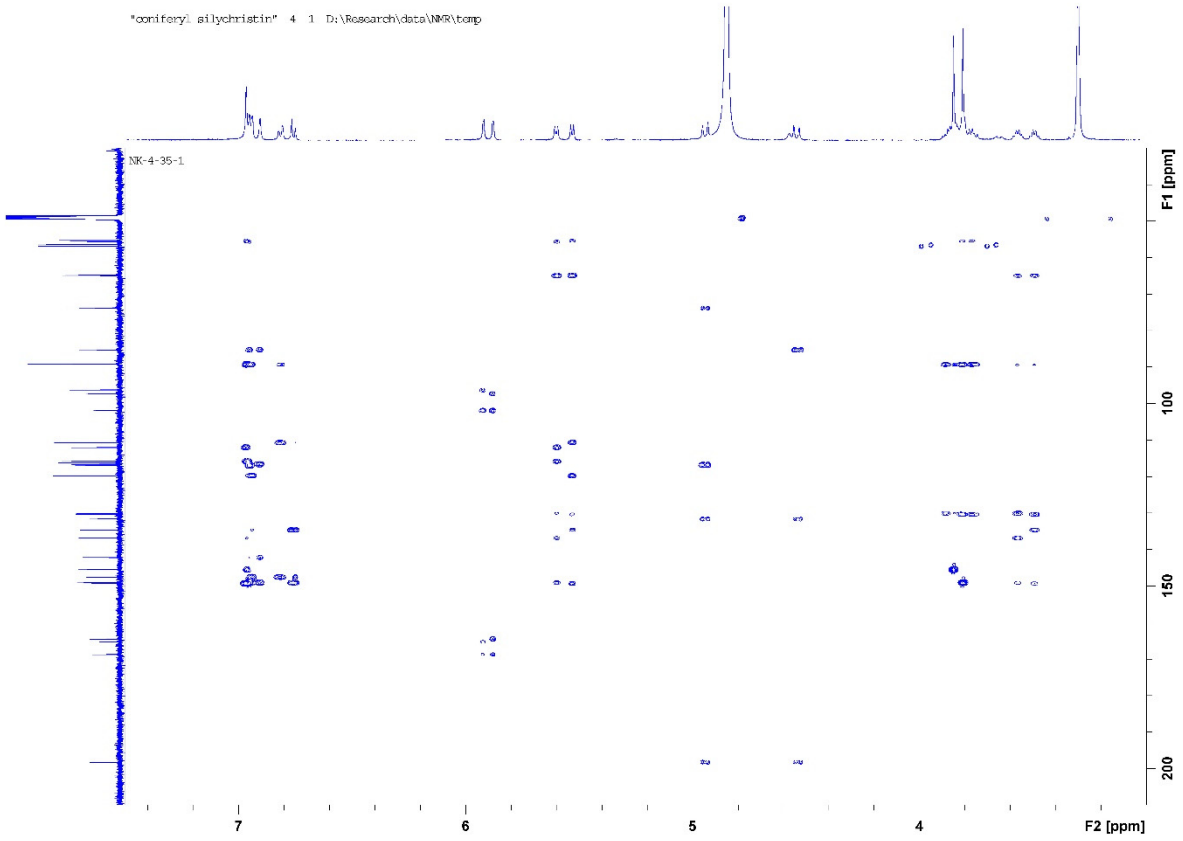

Figure S9. HMBC spectrum of coniferylsilychristin (**4**)

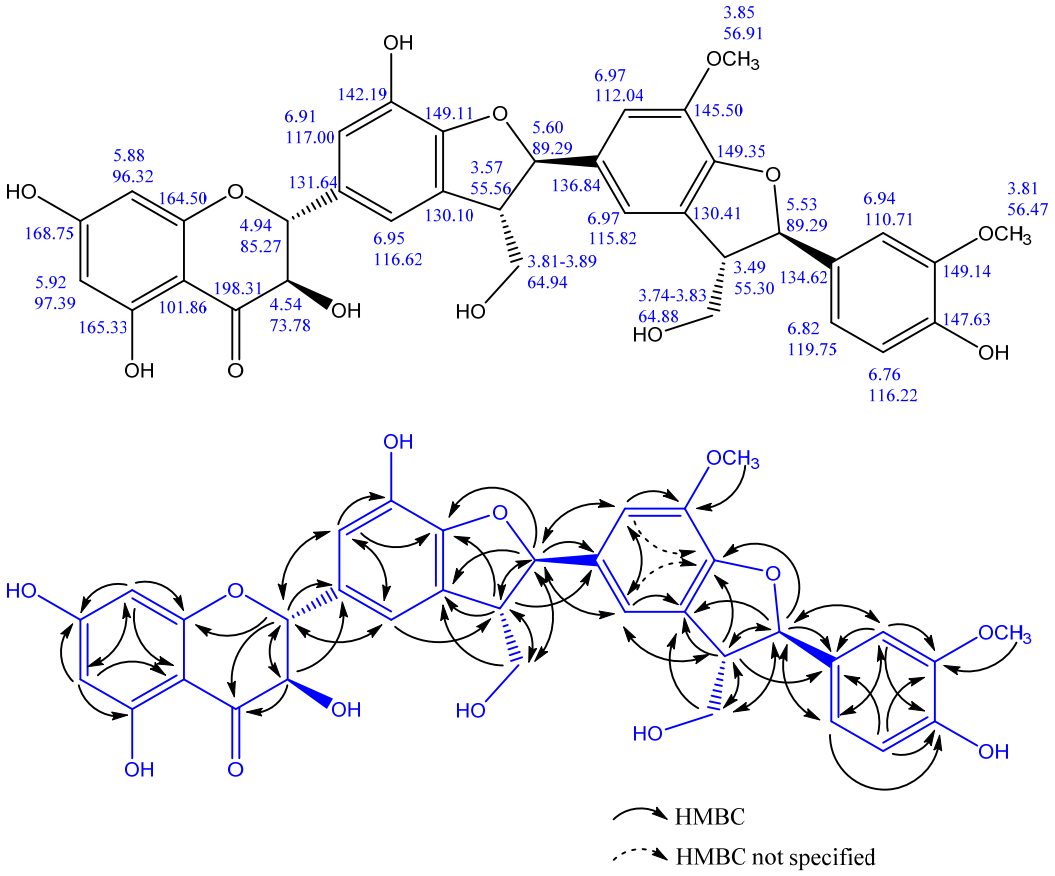

Figure S10. Shifts and HMBC correlations of coniferylsilychristin (**4**)

8-Dehydrodiconiferylsilychristin (5)

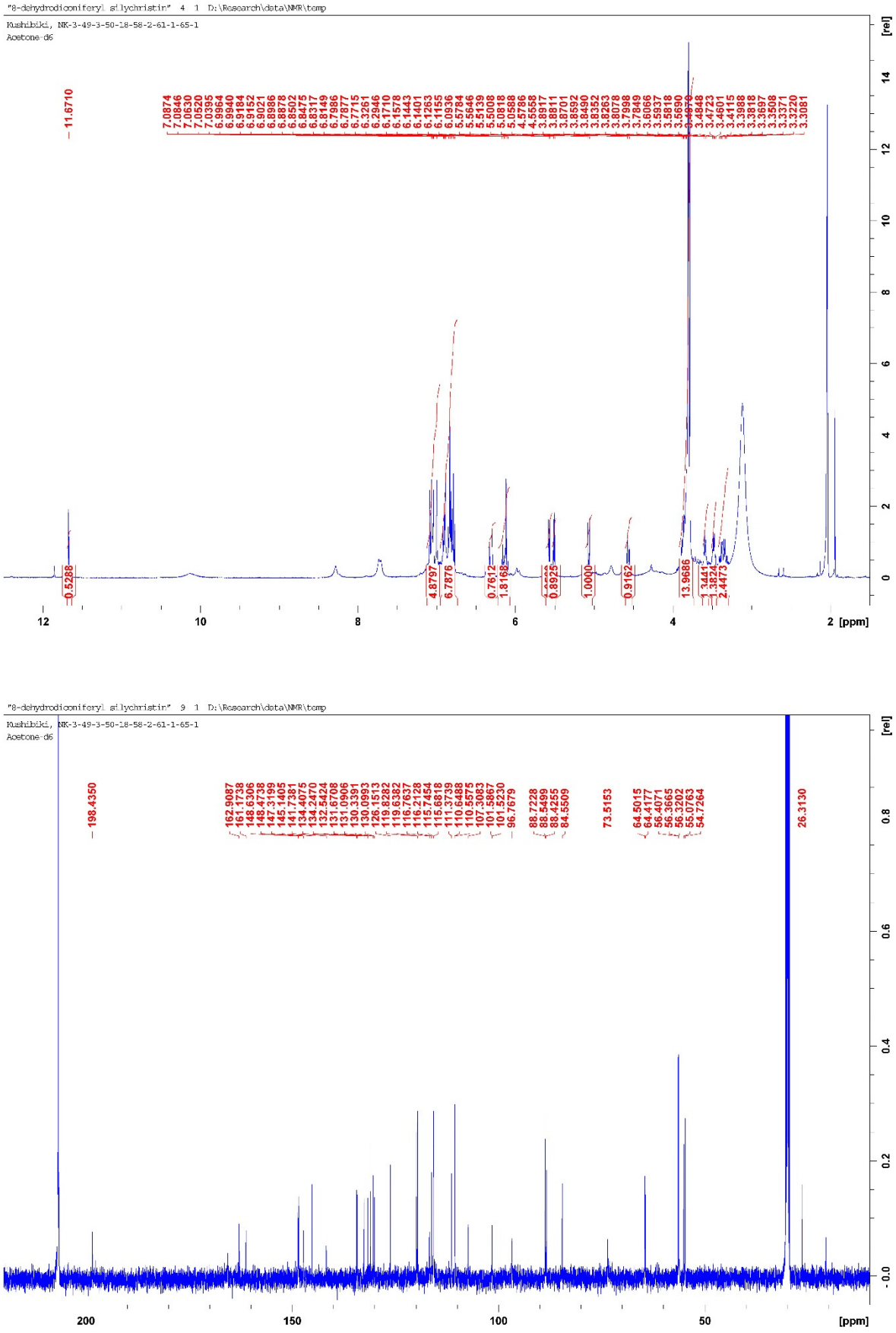

Figure S11. ^{1}H, ^{13}C-NMR spectrum of 8-dehydrodiconiferylsilychristin (**5**)

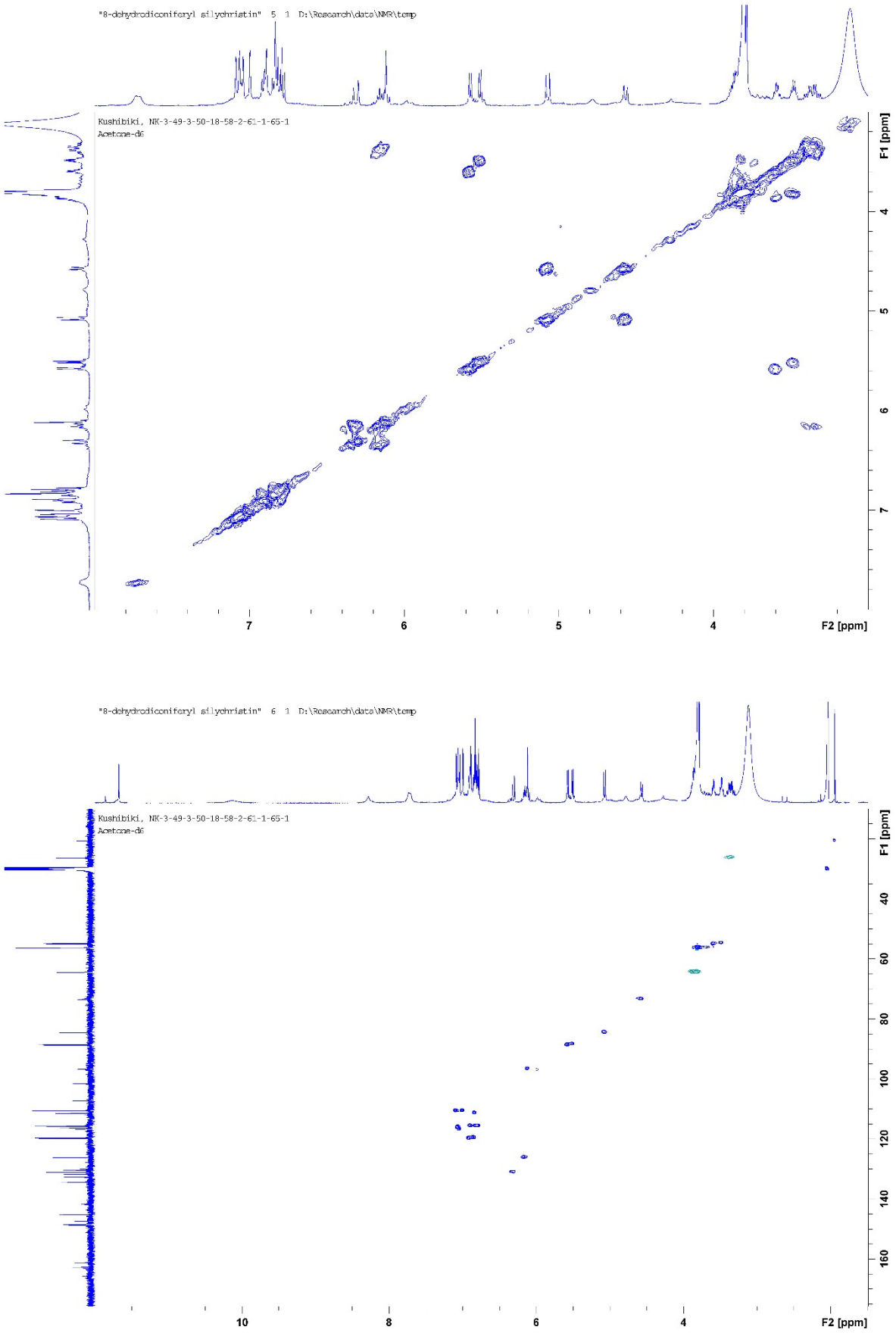

Figure S12. H-H COSY, HSQC spectrum of 8-dehydrodiconiferylsilychristin (**5**)

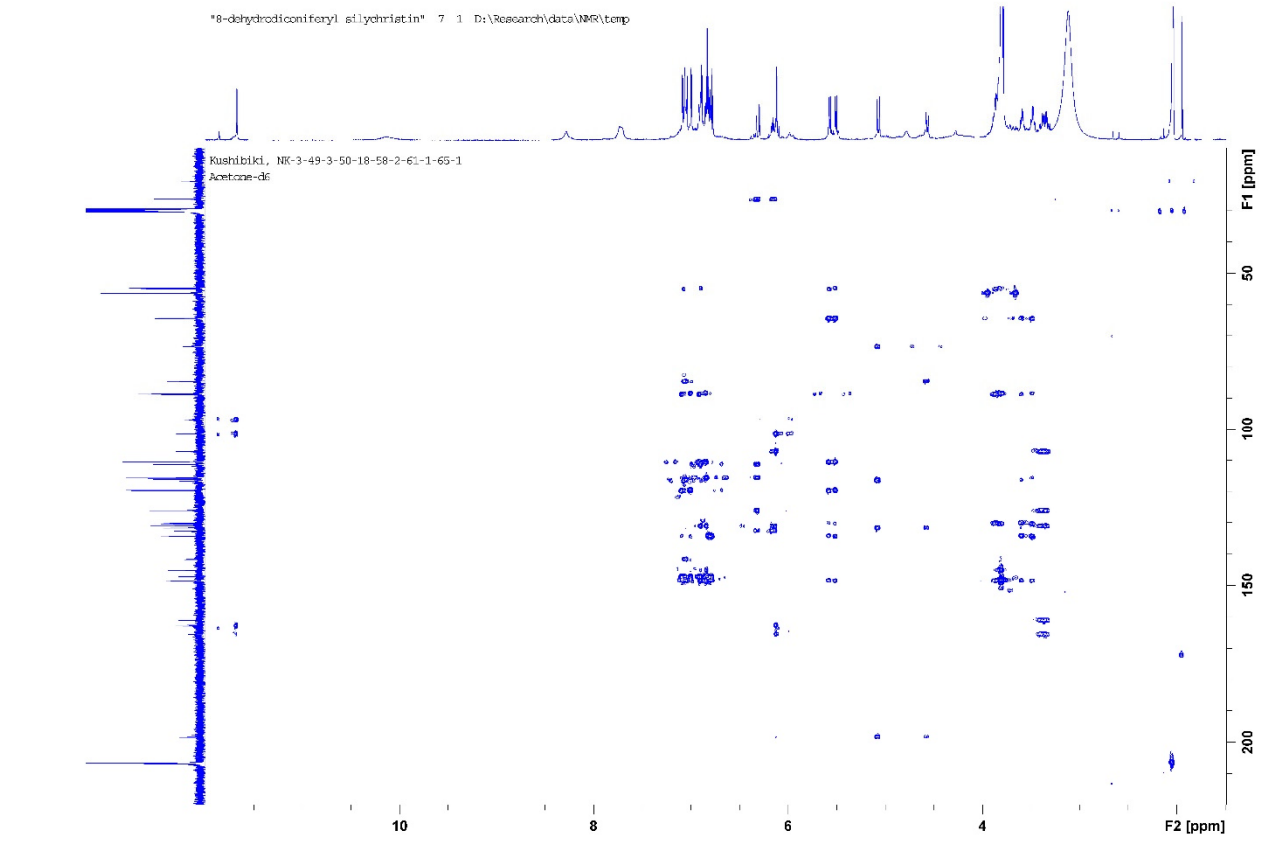

Figure S13. HMBC spectrum of 8-dehydrodiconiferylsilychristin (**5**)

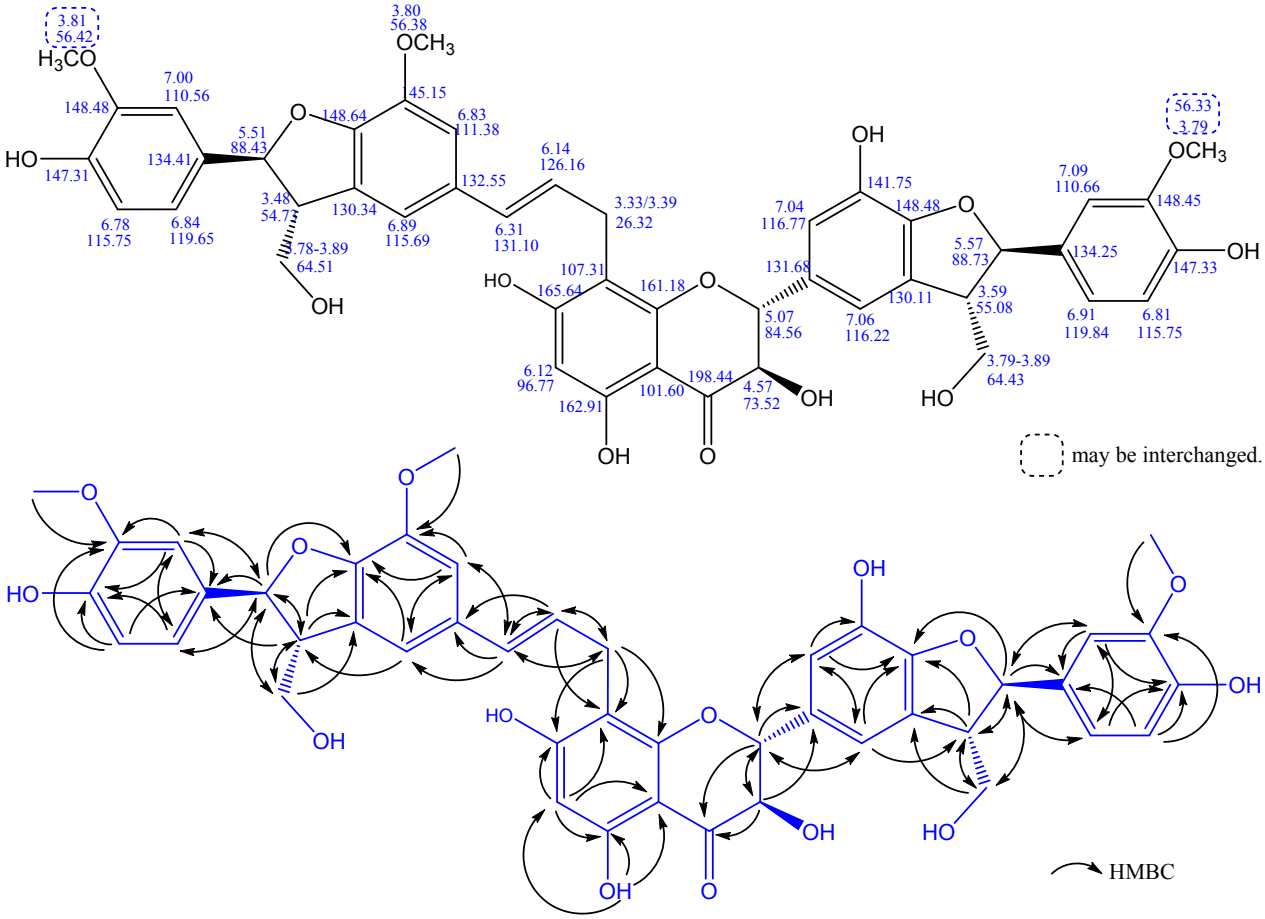

Figure S14. Shifts and HMBC correlations of 8-dehydrodiconiferylsilychristin (**5**)

6-Dehydrodiconiferylsilychristin (6)

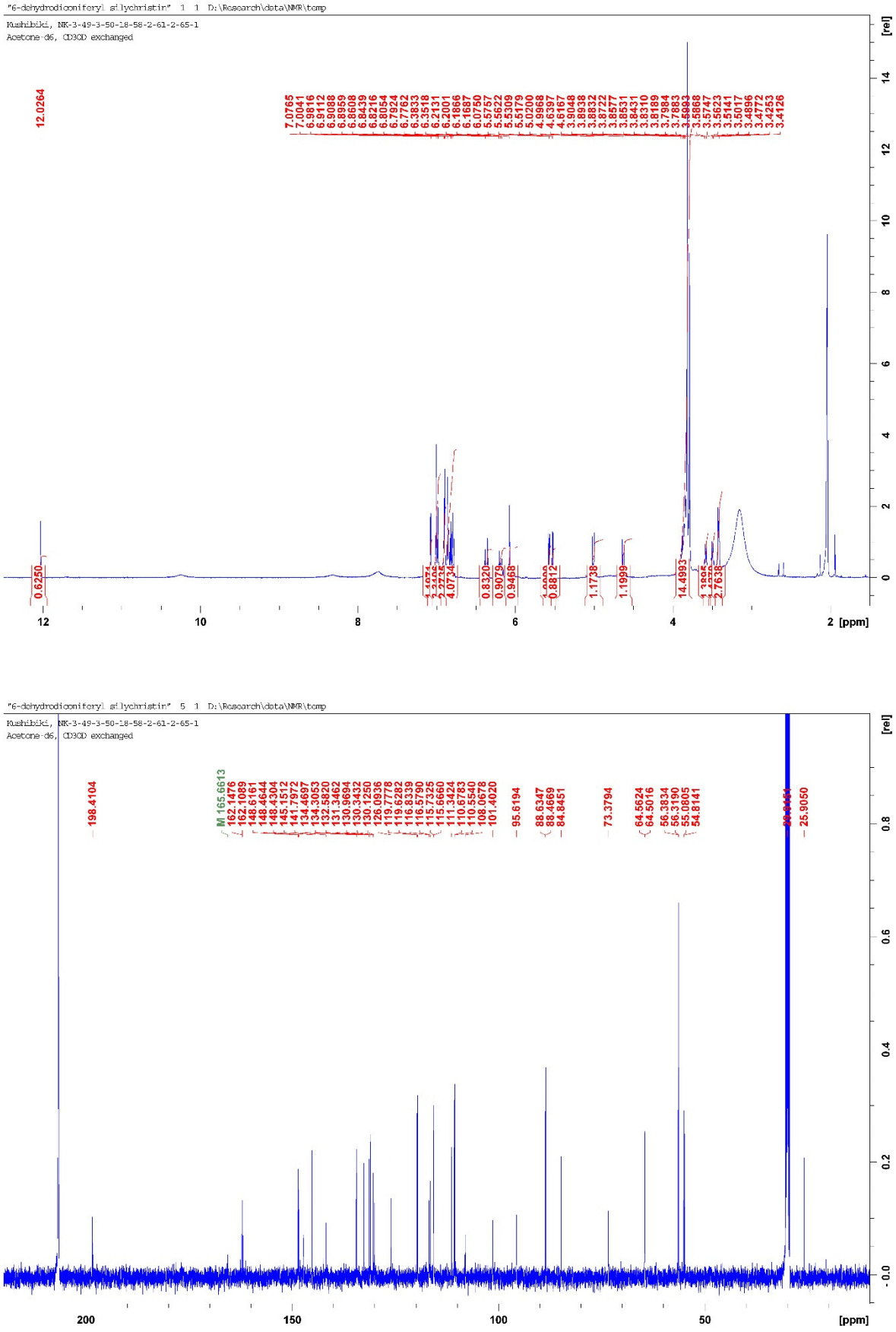

Figure S15. ^{1}H, ^{13}C-NMR spectrum of 6-dehydrodiconiferylsilychristin (**6**)

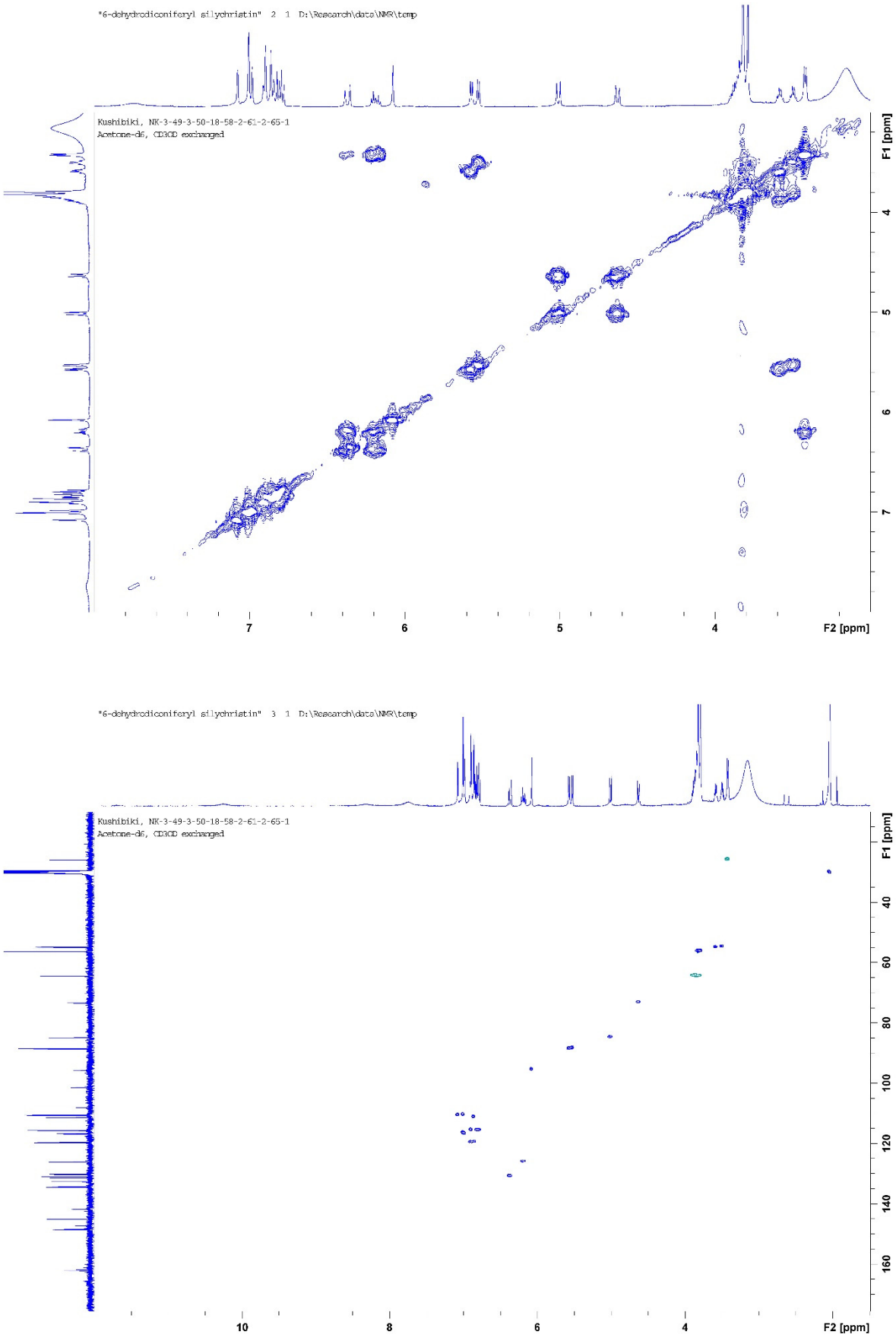

Figure S16. H-H COSY, HSQC spectrum of 6-dehydrodiconiferylsilychristin (**6**)

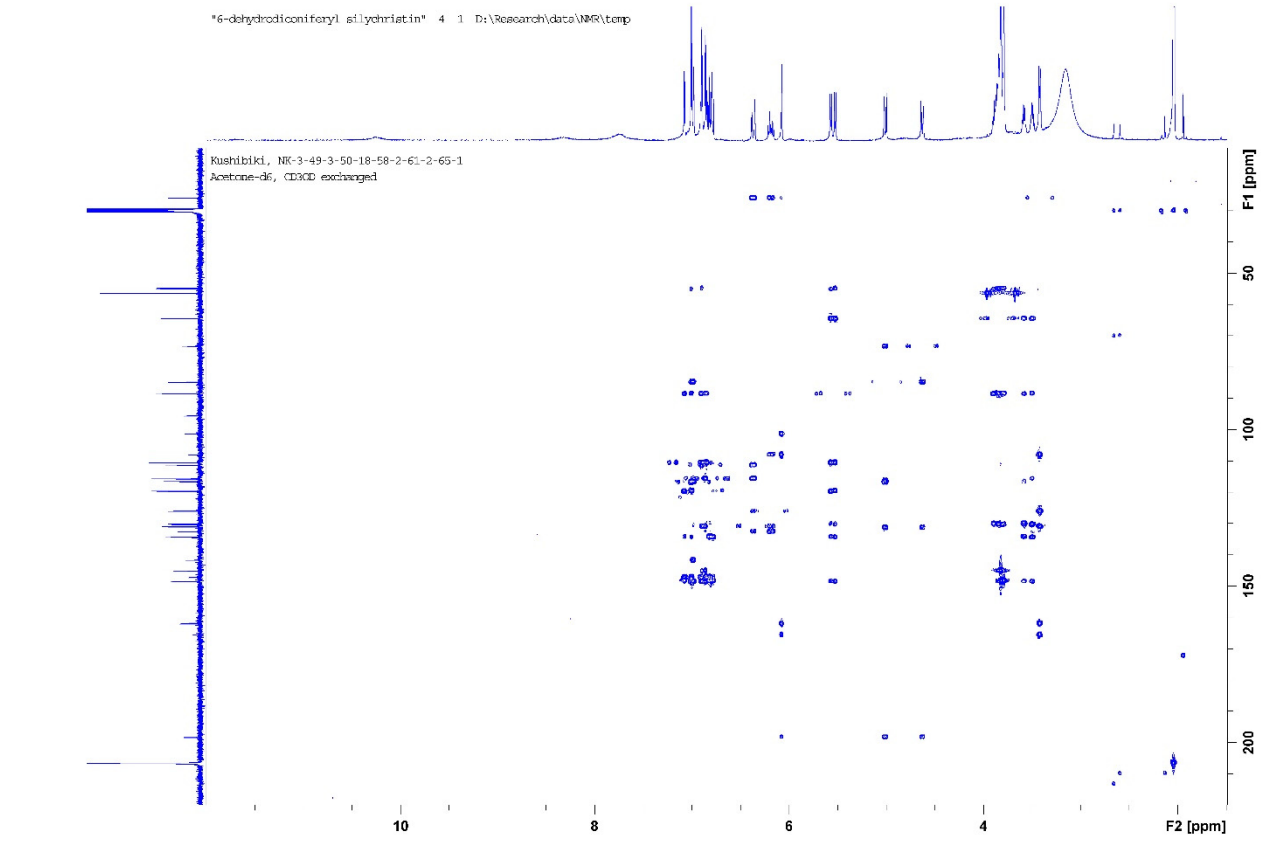

Figure S17. HMBC spectrum of 6-dehydrodiconiferylsilychristin (**6**)

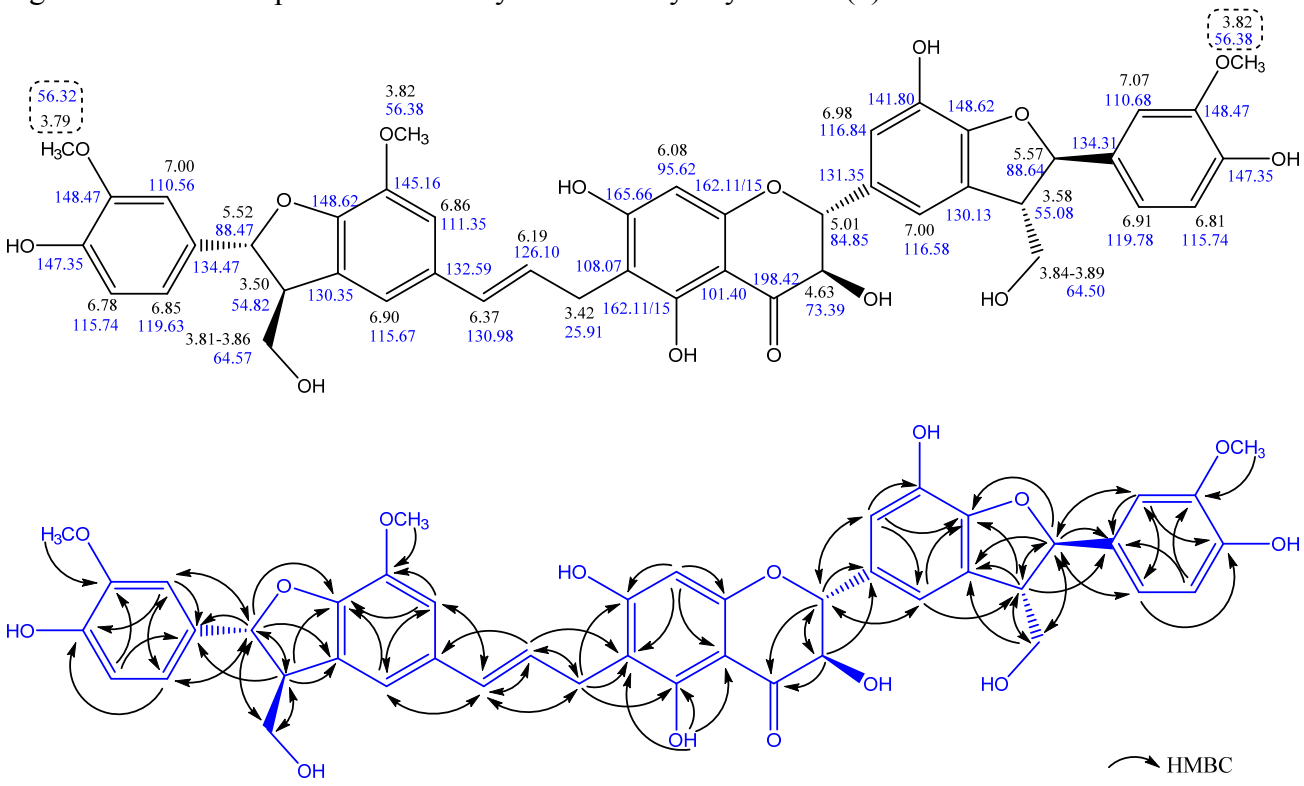

Figure S17. Shifts and HMBC correlations of 6-dehydrodiconiferylsilychristin (**6**)

References

Cheng X-R, Jie R, Wang C-H, Guan B, Jin H-Z, Zhang W-D. 2013. Chemical Constituents from Inula wissmanniana. Chem Nat Compd. 49:815–818.

Choudhary MI, Begum A, Abbaskhan A, Musharraf SG, Ejaz A, Atta-ur-Rahman. 2008. Two New Antioxidant Phenylpropanoids from Lindelofia stylosa. Chem Biodivers. 5:2676–2683.

Qin N bo, Jia C cui, Xu J, Li D hong, Xu F xing, Bai J, Li Z lin, Hua H ming. 2017. New amides from seeds of Silybum marianum with potential antioxidant and antidiabetic activities. Fitoterapia. 119:83–89.